Noncentrosymmetric Lamellar Phase in Blends of ABC Triblock and ac Diblock Copolymers

Robert A. Wickham and An-Chang Shi*

Department of Physics and Astronomy, McMaster University, Hamilton, Ontario L8S 4M1, Canada

Received April 6, 2001; Revised Manuscript Received June 15, 2001

ABSTRACT: The phase behavior of blends of ABC triblock and ac diblock copolymers is examined using self-consistent mean-field theory. Several equilibrium lamellar structures are observed, depending on the volume fraction of the diblocks, $\bar{\phi}_2$, the monomer interactions, and the degrees of polymerization of the copolymers. For segregations just above the order−disorder transition the triblocks and diblocks mix together to form centrosymmetric lamellae. As the segregation is increased, the triblocks and diblocks spatially separate either by macrophase-separating or by forming a noncentrosymmetric (NCS) phase of alternating layers of triblock and diblock (...ABCcaABCca...). The NCS phase is stable over a narrow region near $\bar{\phi}_2 = 0.4$. This region is widest near the critical point on the phase coexistence curve and narrows to terminate at a triple point at higher segregation. Above the triple point there is two-phase coexistence between almost pure triblock and diblock phases. The theoretical phase diagram is consistent with experiments.

I. Introduction

Materials that lack a center of symmetry in the absence of a polarizing field are rare in nature and have attracted much recent interest.[1−4] These noncentrosymmetric (NCS) materials can exhibit dipolar second-order nonlinear optical activity (second-harmonic generation),[2,3] in addition to piezoelectricity and pyroelectricity,[2] without the need to apply a polarizing field. As such, NCS materials are of great technological interest. Recently, the capability to make NCS structures in block copolymer blends has been demonstrated experimentally.[4] Block copolymers consist of two (or more) chains, or blocks, of chemically distinct monomers covalently bonded end-to-end to form a single polymer. Competition between the repulsion of unlike blocks and the constraint that the blocks are attached together leads to the formation of ordered periodic structures. Block copolymers are promising materials to use in the design of NCS structures due to the high degree of control one has over the structure and properties of the blocks. NCS structures created using polymers have longer periods than those created previously using small molecules.[2,3] The periodicity of the structure can be changed by adjusting the block size, creating the potential to tune the wavelengths for second-harmonic generation. The dielectric properties of the blocks can be tailored to the desired application. Finally, block copolymers self-assemble into periodic NCS structures, so no microscale fabrication techniques are necessary to produce the NCS structure.

The key breakthrough in ref 4 that made possible the formation of NCS structures in block copolymers was the recognition that blends of ABC triblock copolymers and ac diblock copolymers, instead of pure melts of ABC triblock copolymers, are required.[5] Here A, B, and C refer to the chemical species of each block—the a and c blocks on the diblock are the same chemical species as the A and C blocks on the triblock. Pure ac diblock melts produce stable lamellar, hexagonally packed cylindrical, body-centered-cubic, and gyroid phases, all of which have centers of symmetry. Pure ABC triblock melts have an even richer phase diagram (see refs 6 and 7 for a discussion), but almost all of the phases so far discovered are centrosymmetric.[8] Compared to the pure phases, the behavior of blends of triblocks and diblocks is relatively unexplored and is a topic of current fundamental interest.

In ref 4 only lamellar structures were reported, and we will restrict the discussion to lamellar structures in this paper. As discussed in refs 4 and 9 and shown here in Figure 1, possible lamellar structures in blends of ABC triblock and ac diblock copolymers include triblock-rich and diblock-rich phases where the triblock and diblock mix together to form a "mixed" centrosymmetric (MCS) structure, a NCS phase where the triblocks and diblocks spatially separate into alternating triblock and diblock layers (...ABCcaABCca...), a centrosymmetric double-layer (CSDL) phase of alternating double layers of triblock and diblock (...ABCcaacCBA...),[10] and regions of two-phase coexistence between these phases.[11] When it is favorable for the triblocks and diblocks to spatially separate, it is unclear whether the system will achieve this by forming a structure with alternating triblock and diblock layers or by macrophase separation. However, by carefully tuning the system parameters, the authors of ref 4 were able to find the NCS structure.

Given the complexity of the pure ABC triblock phase diagram, and the even greater complexity of the phase diagram for the blend, a theoretical guide to experimental searches for the NCS structure would be helpful. The two main questions one would like to answer are the following: what is the driving mechanism behind the formation of the NCS phase, and where in phase space should one expect the NCS structure to be stable? To date, the only theoretical studies of these blends are those of Leibler et al.[9] and Birshtein et al.[12] in the strong-segregation limit. These papers focused on answering the first question by explaining the stability of the NCS phase in terms of an entropic advantage to forming mixed aA domains of a and A block (from the diblock and the triblock, respectively), when compared with the formation of AA (and aa) domains (the same

* Corresponding author: e-mail shi@physics.mcmaster.ca.

10.1021/ma010601q CCC: $20.00
Published on Web 08/04/2001

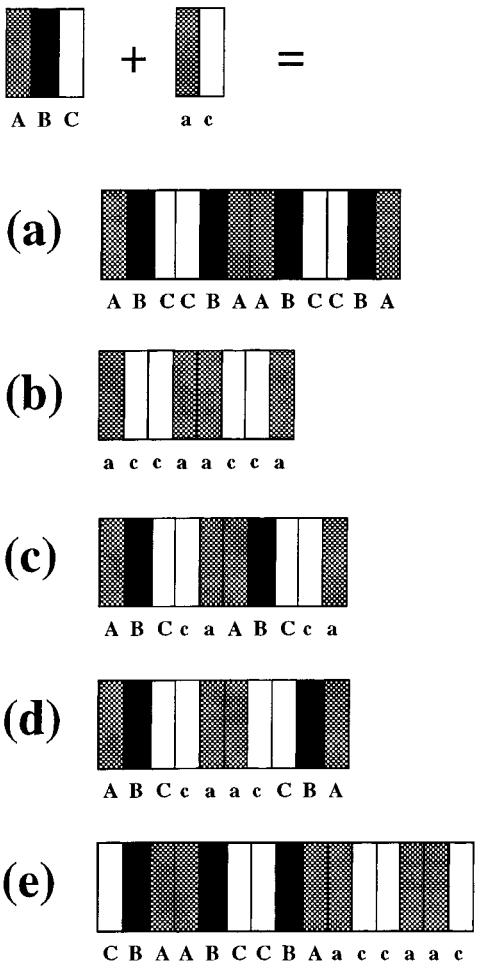

Figure 1. Some possible lamellar structures in a blend of ABC triblock and ac diblock copolymers: (a) triblock-rich mixed centrosymmetric (MCS), (b) diblock-rich mixed centrosymmetric (MCS), (c) noncentrosymmetric (NCS), (d) centrosymmetric double-layer (CSDL), and (e) two-phase coexistence.

arguments apply to mixed cC domains). However, these studies do not directly address the second question. In this paper, we expand the scope of theoretical understanding by examining blends of ABC triblock and ac diblock copolymers using self-consistent mean-field theory. Although this formalism can be used to determine in detail the structure of the aA and cC domains,[13] thereby providing information about the driving mechanism, we do not focus on this here. Rather, our aim is to answer the second question by examining the effect of blend composition on the phase behavior, the possibility for phase separation, and the phase behavior in the weak to intermediate segregation regime.

II. Mean-Field Theory

Consider an incompressible blend of ac diblock copolymers and ABC triblock copolymers in a volume V. The total degree of polymerization of the diblock is N; for the triblock it is ΩN (thus, Ω is the ratio of the triblock degree of polymerization to that of the diblock). The diblock consists of an a-block, with a degree of polymerization $f_{2A}N$, and a c-block, with a degree of polymerization $f_{2C}N$. The diblock composition variables satisfy $f_{2A} + f_{2C} = 1$. Similarly, the triblock consists of three blocks with degrees of polymerization $f_{3\alpha}\Omega N$, where α = A, B, or C. The triblock composition variables satisfy $f_{3A} + f_{3B} + f_{3C} = 1$. We scale distances by the Gaussian radius of gyration of the diblock, $R_{g2} = b(N/6)^{1/2}$. The monomer statistical Kuhn length b and the bulk monomer density ρ_0 are assumed to be the same for all three chemical species. In what follows, we will scale the chain arc-length by the diblock degree of polymerization N.

Beginning with the many-chain Edwards Hamiltonian, we can derive the free energy F of the blend in the mean-field approximation.[14] The suitably scaled free energy density f at temperature T has the form

$$f \equiv \frac{NF}{\rho_0 V k_B T} = \frac{1}{V}\int d\mathbf{r}\, \{\chi_{AB}N\phi_A(\mathbf{r})\,\phi_B(\mathbf{r}) + \chi_{AC}N\phi_A(\mathbf{r})\,\phi_C(\mathbf{r}) + \chi_{BC}N\phi_B(\mathbf{r})\,\phi_C(\mathbf{r}) - \sum_{\alpha=A,B,C}\omega_\alpha(\mathbf{r})\,\phi_\alpha(\mathbf{r})\} - e^{\mu_2}Q_2[\omega] - Q_3[\omega] \quad (1)$$

We derived eq 1 using the grand canonical ensemble.[15] Multiple phase coexistence, which we will encounter below, is most conveniently studied using this ensemble. The three Flory−Huggins interaction parameters χ_{AB}, χ_{AC}, and χ_{BC} are responsible for repulsion between unlike blocks. We denote the volume fraction of α monomers from the n-blocks at position $\mathbf{r}$ as $\phi_{n\alpha}(\mathbf{r})$ and write the volume fraction of α monomers, $\phi_\alpha(\mathbf{r})$, and of diblocks, $\phi_2(\mathbf{r})$, as

$$\phi_\alpha(\mathbf{r}) \equiv \phi_{2\alpha}(\mathbf{r}) + \phi_{3\alpha}(\mathbf{r}) \quad (2)$$

$$\phi_2(\mathbf{r}) \equiv \phi_{2A}(\mathbf{r}) + \phi_{2C}(\mathbf{r}) \quad (3)$$

The chemical potential for the diblocks is μ_2, in units of k_BT. Since the blend is incompressible, the chemical potential for the triblocks can be set to zero without loss of generality.

In eq 1, $Q_2[\omega]$ is the partition function of a single diblock copolymer interacting with the mean fields $\omega_\alpha(\mathbf{r})$. Similarly, $Q_3[\omega]$ is the partition function of a single triblock copolymer interacting with these mean fields. These partition functions may be written in terms of the propagators $Q_\alpha(\mathbf{r},s|\mathbf{r}')$, which give the probability that the α monomer at arc length s is at position $\mathbf{r}$, given that the α monomer at arc length 0 is at $\mathbf{r}'$:

$$Q_2[\omega] = \frac{1}{V}\int d\mathbf{r}_1\, d\mathbf{r}_2\, d\mathbf{r}_3\, Q_A(\mathbf{r}_1, f_{2A}|\mathbf{r}_2)\, Q_C(\mathbf{r}_2, f_{2C}|\mathbf{r}_3) \quad (4)$$

$$Q_3[\omega] = \frac{1}{V}\int d\mathbf{r}_1\, d\mathbf{r}_2\, d\mathbf{r}_3\, d\mathbf{r}_4\, Q_A(\mathbf{r}_1, f_{3A}\Omega|\mathbf{r}_2)\, Q_B(\mathbf{r}_2, f_{3B}\Omega|\mathbf{r}_3)\, Q_C(\mathbf{r}_3, f_{3C}\Omega|\mathbf{r}_4) \quad (5)$$

The factors of $1/V$ are inserted above for convenience. The propagators satisfy the modified diffusion equation

$$\frac{\partial}{\partial s}Q_\alpha(\mathbf{r},s|\mathbf{r}') = \nabla^2_{\mathbf{r}}Q_\alpha(\mathbf{r},s|\mathbf{r}') - \omega_\alpha(\mathbf{r})\,Q_\alpha(\mathbf{r},s|\mathbf{r}') \quad (6)$$

with the initial condition

$$Q_\alpha(\mathbf{r},0|\mathbf{r}') = \delta(\mathbf{r} - \mathbf{r}') \quad (7)$$

In the mean-field approximation the fields ω_α are related to the monomer volume fractions through the relations

$$\omega_A(\mathbf{r}) = \chi_{AB}N\phi_B(\mathbf{r}) + \chi_{AC}N\phi_C(\mathbf{r}) + \eta(\mathbf{r}) \quad (8)$$

$$\omega_B(\mathbf{r}) = \chi_{AB}N\phi_A(\mathbf{r}) + \chi_{BC}N\phi_C(\mathbf{r}) + \eta(\mathbf{r}) \quad (9)$$

$$\omega_C(\mathbf{r}) = \chi_{AC}N\phi_A(\mathbf{r}) + \chi_{BC}N\phi_B(\mathbf{r}) + \eta(\mathbf{r}) \quad (10)$$

where the field η is to be adjusted to enforce the incompressibility condition

$$\phi_A(\mathbf{r}) + \phi_B(\mathbf{r}) + \phi_C(\mathbf{r}) = 1 \quad (11)$$

The monomer volume fractions are, in turn, related to functional derivatives of $Q_2[\omega]$ and $Q_3[\omega]$:

$$\phi_{2\alpha}(\mathbf{r}) = -Ve^{\mu_2}\frac{\delta Q_2[\omega]}{\delta\omega_\alpha(\mathbf{r})} \quad (12)$$

$$\phi_{3\alpha}(\mathbf{r}) = -V\frac{\delta Q_3[\omega]}{\delta\omega_\alpha(\mathbf{r})} \quad (13)$$

These functional derivatives are evaluated using eqs 4−7.

To obtain the *exact* mean-field solution for a given point in parameter space, eqs 8−13 need to be solved self-consistently using numerical methods. The method of solution involves selecting a set of basis functions appropriate to the space group of the periodic structure to be examined and reformulating the theory in the reciprocal space of these basis functions.[16] With initial guesses for the periodicity, D, and monomer profiles, ϕ_α, of the structure, the reciprocal space versions of eqs 8−13 are solved iteratively to obtain the mean-field profiles and free energy density f corresponding to the chosen D. This procedure is repeated for different choices of D until the free energy density is minimized at the system's preferred periodicity. The numerical procedure and the reciprocal space formulation are discussed in more detail in refs 16−18. The preferred periodicity and minimal free energy density are determined for all possible structures. These free energy densities are compared, and the structure with the lowest f at a given point in phase space is the equilibrium structure at that point. In the $f-\mu_2$ plane, two-phase coexistence occurs when the free energy density curves for two structures cross at a given value of μ_2. Three-phase coexistence occurs when three such curves intersect at a point. Even though we compare free energy density curves as a function of μ_2, when we plot phase diagrams, we use the average diblock volume fraction, $\bar{\phi}_2$, as a variable, instead of its thermodynamic conjugate, μ_2.[19]

A pure triblock copolymer melt can form many different periodic structures.[6,7] The number of structures formed by blending triblock copolymers with diblock copolymers is even more diverse. In this paper, we restrict ourselves to discussing lamellar structures, since they have been the subject of experimental investigations of noncentrosymmetry.[4] The problem is then one-dimensional with cosines and sines as basis functions. The monomer volume fractions and the mean fields for a lamellar modulation chosen to be along the z-axis are written as

$$\phi_\alpha(z) = \sum_{n=0}^{\infty}\phi_{\alpha,n}^{(c)}\cos\left(\frac{2\pi n}{D}z\right) + \sum_{n=1}^{\infty}\phi_{\alpha,n}^{(s)}\sin\left(\frac{2\pi n}{D}z\right) \quad (14)$$

$$\omega_\alpha(z) = \sum_{n=0}^{\infty}\omega_{\alpha,n}^{(c)}\cos\left(\frac{2\pi n}{D}z\right) + \sum_{n=1}^{\infty}\omega_{\alpha,n}^{(s)}\sin\left(\frac{2\pi n}{D}z\right) \quad (15)$$

where $\phi_{\alpha,n}^{(c)}$ and $\phi_{\alpha,n}^{(s)}$ are the Fourier amplitudes of the cosines and sines, respectively, for the monomer volume fractions; $\omega_{\alpha,n}^{(c)}$ and $\omega_{\alpha,n}^{(s)}$ have a similar meaning for the mean fields. These amplitudes are determined self-consistently from eqs 8−13 using the method mentioned in the preceding paragraph. The noncentrosymmetric phase was obtained using both sines and cosines and an initial monomer profile that was NCS (...ABCca...) to begin the iteration procedure. Centrosymmetric phases have only cosines as basis functions ($\phi_{\alpha,n}^{(s)} = \omega_{\alpha,n}^{(s)} = 0\ \forall\ \alpha, n$). The MCS structure was found at about the period of the NCS structure. A centrosymmetric double-layer structure was found at about twice the NCS period, using the sequence (...ABCcaacCBA...) as an initial profile for the iteration step. In the numerical computation the number of basis functions used in the expansions given by eqs 14 and 15 is finite. As more basis functions are used, the value obtained for the free energy density of a given structure at a given point in phase space becomes more accurate. The number of basis functions in our computation of the free energy density, which is $O(1)$, is selected to achieve an accuracy of 10^{-6}, which is more than sufficient to resolve the small differences in free energy between the various phases. As the blend segregation increases, the interfaces become sharper and more basis functions are needed to achieve this accuracy.[20]

III. Results and Discussion

Since the parameter space for this system is large—$\chi_{AB}N$, $\chi_{AC}N$, $\chi_{BC}N$, Ω, f_{2A}, f_{3A}, f_{3B}, and $\bar{\phi}_2$ can all be varied independently—we have to be careful to select parameters that favor a stable lamellar phase. A stable lamellar phase is most likely when the block compositions are symmetric, $f_{2A} = {}^1/_2$, $f_{3A} = f_{3B} = {}^1/_3$, and the Flory−Huggins interaction parameters are equal, $\chi_{AB} = \chi_{AC} = \chi_{BC} \equiv \chi$. Accordingly, we fix the block compositions to be symmetric and examine only situations where the Flory−Huggins interaction parameters are equal or nearly equal. Even within these bounds, the phase behavior of the blend is rich.

The phase diagram in the $\chi N-\bar{\phi}_2$ plane, for the case where all the Flory−Huggins interaction parameters are equal, is shown in Figure 2. The ratio of triblock to diblock lengths is $\Omega = 1.5$. At the lowest values of χN the blend is disordered. As χN increases, there is a transition to a mixed centrosymmetric (MCS) phase where the triblocks and diblocks mix together uniformly but form a lamellar phase.[21] If $\bar{\phi}_2$ is small and the blend is triblock-rich, the lamellar structure will be alternating triblock layers (...ABCCBA...), as in Figure 1a. As $\bar{\phi}_2$ increases, the blend becomes diblock-rich and the structure becomes alternating diblock layers (...acca...), as in Figure 1b. A typical monomer density profile for the MCS phase is shown in Figure 3.

For larger values of χN (in the intermediate segregation regime around $\chi N \approx 14$) the B block tends to expel the diblock a and c blocks from its domain, and it becomes favorable for the triblocks and diblocks to spatially separate. The transition from mixed to spatially separated states is indicated by the phase coexistence line in Figure 2. Above the transition, the existence

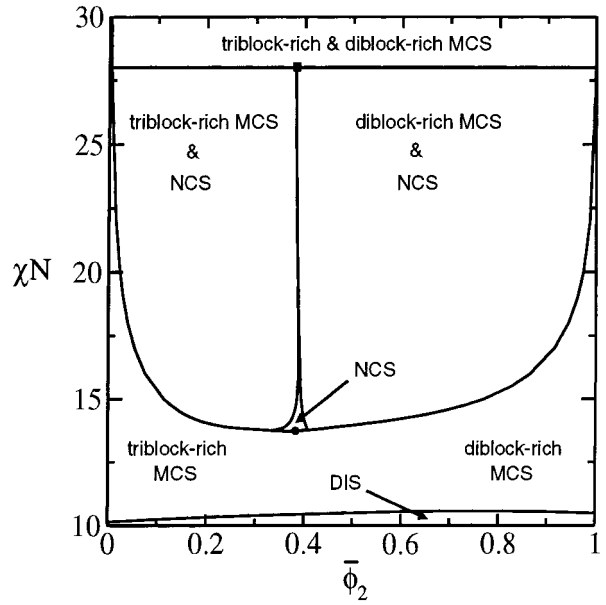

Figure 2. Phase diagram in the $\chi N-\bar{\phi}_2$ plane, for the case where all the Flory−Huggins interaction parameters are equal ($\chi_{AB} = \chi_{AC} = \chi_{BC} \equiv \chi$). The triblock to diblock length ratio is $\Omega = 1.5$. The labels are as follows: DIS = disordered; MCS = mixed centrosymmetric; NCS = noncentrosymmetric. Below the phase coexistence line, the MCS phase goes from being triblock-rich to diblock-rich, as the average diblock volume fraction $\bar{\phi}_2$ increases. The critical point for the MCS to NCS transition is indicated by a solid circle. The narrow region of NCS phase stability terminates at a triple point, indicated by a solid square. Regions of two-phase coexistence are indicated. Above the horizontal line at $\chi N \approx 28$ there is two-phase coexistence between an almost pure triblock phase and an almost pure diblock phase.

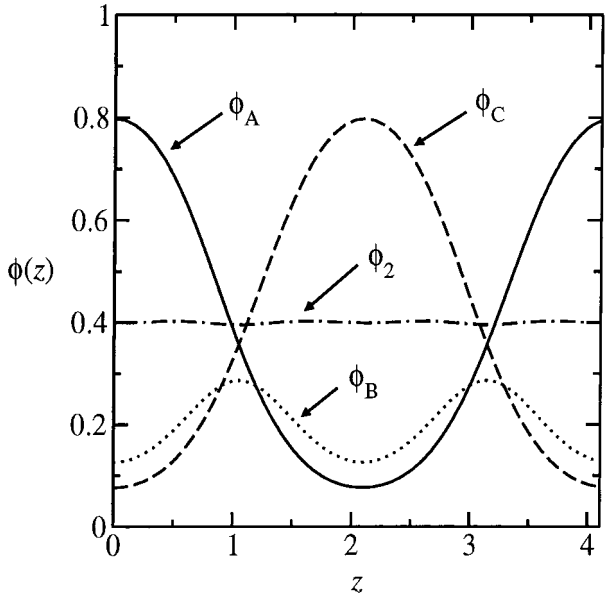

Figure 3. Profile of one period of the MCS lamellar phase for $\chi N = 13$ (all Flory−Huggins interaction parameters are equal), $\bar{\phi}_2 = 0.4$, and $\Omega = 1.5$. The distance perpendicular to the lamellae is z, measured in units of the radius of gyration of the diblock, R_{g2}.

of a stable NCS phase of alternating triblock and diblock layers (...ABCca... as in Figure 1c) in a narrow region around $\bar{\phi}_2 \approx 0.4$ prevents the system from phase-separating into coexisting triblock-rich and diblock-rich phases. Instead, for values of $\bar{\phi}_2$ lower than the stability region for the NCS phase, the triblock-rich phase

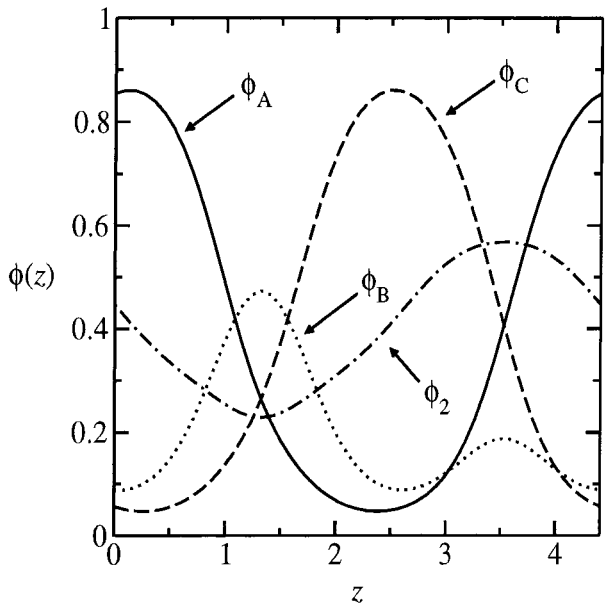

Figure 4. Profile of one period of the NCS lamellar phase for $\chi N = 14$ (all Flory−Huggins interaction parameters are equal), $\bar{\phi}_2 = 0.4$, and $\Omega = 1.5$. The distance perpendicular to the lamellae is z, measured in units of the radius of gyration of the diblock, R_{g2}.

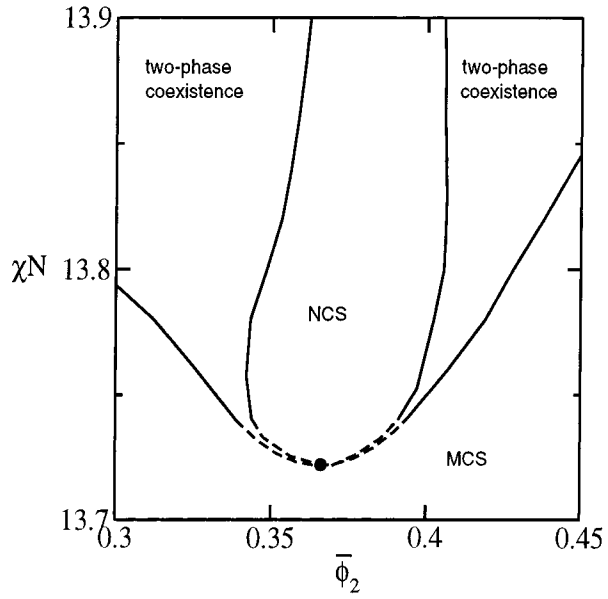

Figure 5. Region in Figure 2 near the critical point in more detail. The parameters and notation are the same as in Figure 2. The dashed curves are extrapolations of the phase boundaries.

coexists with the NCS phase, while for values of $\bar{\phi}_2$ higher than this stability region the NCS phase coexists with the diblock-rich phase. The volume fraction of each coexisting phase is given by the lever rule. As $\bar{\phi}_2$ increases and the longer triblocks are removed, the periodicity D of the structure decreases. Thus, for a given χN, the triblock-rich MCS phase has a longer period than the NCS phase, and the NCS phase has a longer period than the diblock-rich MCS phase. A typical monomer density profile for the NCS phase is shown in Figure 4.

The widest region of NCS stability occurs near the bottom of the phase-coexistence curve. Figure 5 shows this region in more detail. The phase boundaries appear to converge at a point where $\bar{\phi}_2 \approx 0.365$ and $\chi N \approx 13.72$.

Since the free energy differences between the structures become very small near this point and the NCS phase is only slightly stable with respect to the MCS phase, it becomes difficult to numerically compute the phase boundaries in this region. The dashed curves in Figure 5 are thus extrapolations of the phase boundaries. Given the fact that the free energies of the structures appear to merge at this point and the fact that the difference between the period of the stable NCS and the metastable MCS structure approaches zero as this point is approached, we believe that the point of convergence is a second-order critical point. The order parameter for this transition is the amplitude of the odd-parity basis functions (sines) for the monomer profiles.

When $\chi N > 17$, the region of NCS stability narrows to a sliver, as shown in Figure 2. The NCS stability region terminates at a triple point at $\bar{\phi}_2 \approx 0.381$ and $\chi N \approx 28.0$ where the triblock-rich, diblock-rich, and NCS phases coexist. For larger values of χN the NCS phase is unstable, and there is only two-phase coexistence between almost pure triblock and diblock phases. This part of the phase diagram is similar to the phase diagram of a eutectic material, where a liquid phase (here the NCS phase) intervenes between two solid phases (here the MCS phases) and terminates at an eutectic point (here the triple point).[22]

We have slightly varied the relative values of the Flory–Huggins interaction parameters and examined the effects on the phase diagram. To try to avoid nonlamellar phases, we have kept the interactions in the triblock symmetric ($\chi_{AB} = \chi_{BC}$) and examined the effect of having only slightly weaker repulsion between the middle and outer blocks ($\chi_{AB} = \chi_{BC} = 0.8\chi_{AC}$) and only slightly stronger repulsion between these blocks ($\chi_{AB} = \chi_{BC} = 1.1\chi_{AC}$). The value $\Omega = 1.5$ is used. It is known, however, that for large variations in the Flory–Huggins interaction parameters nonlamellar phases may arise (such as B cylinders or spheres on AC interfaces when $\chi_{AB} = \chi_{BC} > \chi_{AC}$).[6]

In Figure 6 the phase diagram in the $\chi_{AC}N-\bar{\phi}_2$ plane is shown for the case where $\chi_{AB} = \chi_{BC} = 0.8\chi_{AC}$. The overall structure of the phase diagram is the same as in Figure 2 where the Flory–Huggins interaction parameters were equal. (To emphasize the region around the critical point, we only show the lower part of the phase diagram in Figure 6.) The region of NCS stability is shifted to slightly higher values of $\bar{\phi}_2$. More noticeably, the phase coexistence line is shifted to higher values of $\chi_{AC}N$. The critical point now occurs at $\bar{\phi}_2 \approx 0.414$ and $\chi_{AC}N \approx 16.79$, and the triple point occurs at $\bar{\phi}_2 \approx 0.391$ and $\chi_{AC}N \approx 48$. Since the repulsion between the B block and the diblock a and c blocks drives the triblocks and diblocks to spatially separate, decreasing this repulsion raises the phase coexistence line. In Figure 7 the phase diagram in the $\chi_{AC}N-\bar{\phi}_2$ plane is shown for the case where $\chi_{AB} = \chi_{BC} = 1.1\chi_{AC}$. Again, the basic structure of the phase diagram is unchanged from Figure 2, while the phase coexistence line is shifted to lower values of $\chi_{AC}N$. The region of NCS stability is shifted to slightly lower values of $\bar{\phi}_2$. The critical point occurs at $\bar{\phi}_2 \approx 0.350$ and $\chi_{AC}N \approx 12.69$, and the triple point occurs at $\bar{\phi}_2 \approx 0.376$ and $\chi_{AC}N \approx 23$. The increased repulsion between the B block and the diblock a and c blocks drives the triblocks and diblocks to spatially separate at lower values of $\chi_{AC}N$, lowering the phase coexistence line. Interestingly, the phase coexistence line in Figure 7 is more asymmetric than the phase coexistence lines in either Figure 2 or Figure 6. This is due to the increased repulsion of the B block in Figure 7, which accentuates the difference between the triblock and the diblock.

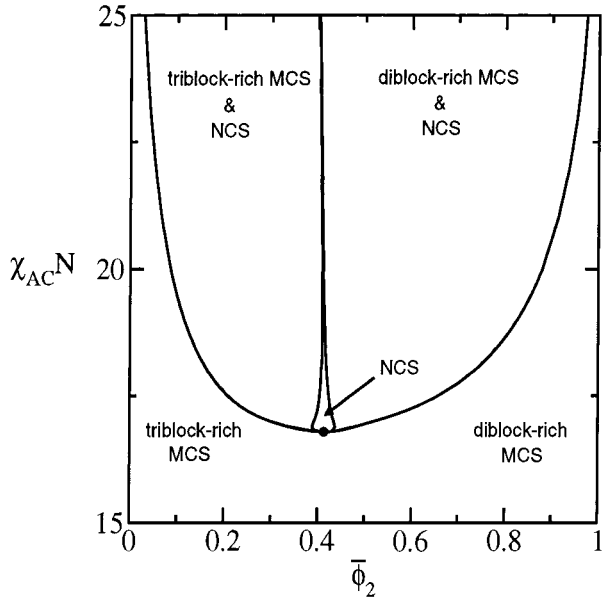

Figure 6. Phase diagram in the $\chi_{AC}N-\bar{\phi}_2$ plane, for the case where $\chi_{AB} = \chi_{BC} = 0.8\chi_{AC}$. The triblock to diblock length ratio is $\Omega = 1.5$. The notation used is the same as in Figure 2. We have chosen to focus on the region of the phase diagram near the critical point. The disordered phase exists below $\chi_{AC}N \approx 10.5$, and the triple point exists for $\chi_{AC}N \approx 48$.

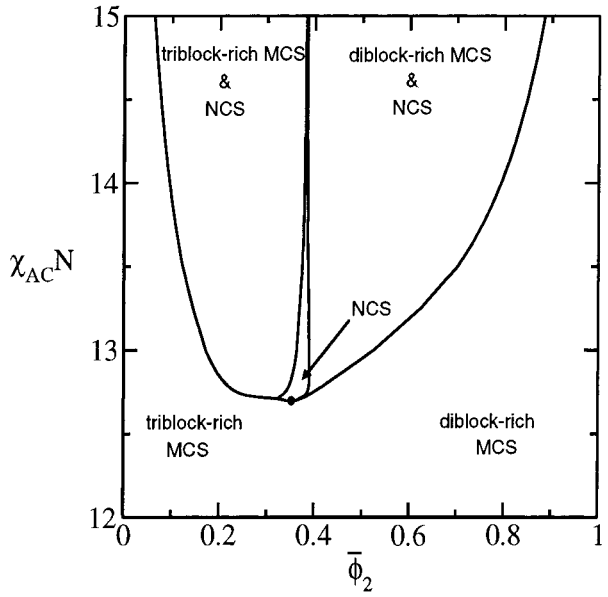

Figure 7. Phase diagram in the $\chi_{AC}N-\bar{\phi}_2$ plane, for the case where $\chi_{AB} = \chi_{BC} = 1.1\chi_{AC}$. The triblock-to-diblock length ratio is $\Omega = 1.5$. The notation used is the same as in Figure 2. We have chosen to focus on the region of the phase diagram near the critical point. The disordered phase exists below $\chi_{AC}N \approx 10.5$, and the triple point exists for $\chi_{AC}N \approx 23$.

It was hoped that by looking at variations in the relative values of the Flory–Huggins interaction parameters the region of NCS stability could be expanded beyond that of Figure 2. In the parameter range we have examined, we have found little, if any, dependence of the width of the NCS stability region on such variations. It appears that, other than an upward (or downward)

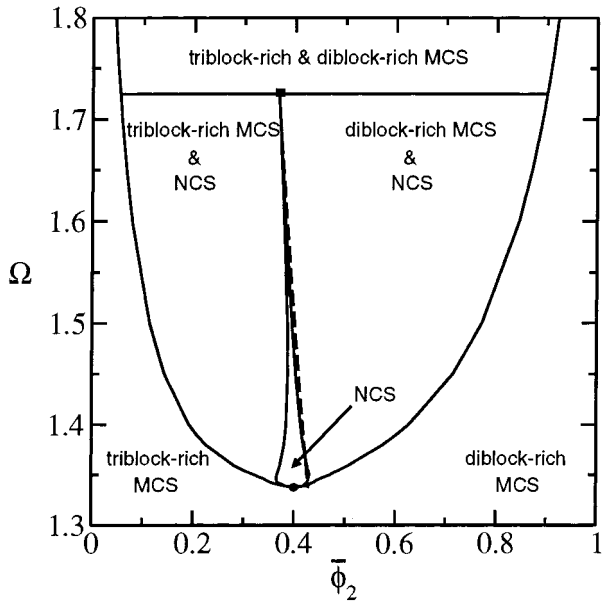

Figure 8. Phase diagram in the $\Omega-\bar{\phi}_2$ plane, for the case where all the Flory−Huggins interaction parameters are equal ($\chi N = 15$). The notation used is the same as in Figure 2. The dashed curve corresponds to eq 16.

shift of the phase coexistence curve and triple point, the structure of the phase diagram is insensitive to slight variations in the relative values of the Flory−Huggins interaction parameters.

To examine the effect of varying the relative degrees of polymerization of the triblocks and diblocks, we show the phase diagram in the $\Omega-\bar{\phi}_2$ plane in Figure 8. In this case, the Flory−Huggins parameters are constant and equal: $\chi N = 15$. Since an increase in the triblock polymerization index results in an increased effective segregation in the triblock, the B block will expel the diblock a and c blocks for large enough Ω. Thus, Figures 2 and 8 are similar. There is a critical point at $\bar{\phi}_2 \approx 0.391$ and $\Omega \approx 1.34$ and a triple point at $\bar{\phi}_2 \approx 0.370$ and $\Omega \approx 1.72$. It is significant that the region of NCS stability slopes to lower $\bar{\phi}_2$ as Ω is increased and that this region roughly corresponds to the condition that the number of diblock copolymers in the blend equals the number of triblock copolymers,

$$\bar{\phi}_2^* = \frac{1}{1+\Omega} \tag{16}$$

Equation 16 is plotted in Figure 8 for comparison. For the phase diagram in Figure 2, where the region of NCS stability is almost vertical, eq 16 with $\Omega = 1.5$ gives $\bar{\phi}_2^* = 0.4$, which is close to what is seen.

We now comment on the stability of the centrosymmetric double-layer (CSDL) phase consisting of alternating triblock and diblock double layers (...ABCcaacCBA...). Naively, one might expect that a flip of every other period of the NCS phase would lead to a periodic structure which is degenerate in free energy with the original NCS phase and has exactly twice the period of the original phase. However, in the phase diagrams shown in Figures 2, 6, 7, and 8 the CSDL structure is metastable. We also observe that the period of the metastable CSDL structure is only approximately twice that of the NCS structure. Below the triple point, in the region where the NCS phase is stable, the CSDL structure has a lower free energy density than the phase-separated state and a higher free energy density than the NCS structure. Above the triple point the CSDL structure has a lower free energy density than the NCS structure but is metastable with respect to two-phase coexistence. The discussion in ref 4 suggests an explanation for the relative stabilities of these structures. Denote the free energy cost to create a domain of type $\alpha\beta$ (= AA, aa, aA, CC, cc, or cC) as $f_{\alpha\beta}$. It is assumed that the system is strongly segregated, so that the penetration of chains from outside the domain can be ignored and domains may be treated as distinct entities. Then, as ref 4 notes, when an AA and an aa domain are replaced by two aA domains, the free energy density changes by the amount $\Delta f_a = 2f_{aA} - (f_{AA} + f_{aa})$. [Similarly, the replacement of CC and cc domains by two cC domains changes the free energy density by $\Delta f_c = 2f_{cC} - (f_{CC} + f_{cc})$.] Examining the structures in Figure 1, we see that the free energy densities, f_{CSDL} of one period of the CSDL phase, f_{NCS} of two periods of the NCS phase, and f_{PS} of the equivalent phase-separated state, are given by

$$f_{CSDL} = \Delta f_c + f_{PS} \tag{17}$$

$$f_{NCS} = \Delta f_a + \Delta f_c + f_{PS} \tag{18}$$

$$f_{PS} = f_{AA} + f_{aa} + f_{CC} + f_{cc} + 2(s_{AB} + s_{CB} + s_{ac}) \tag{19}$$

where $s_{\alpha\beta}$ is the free energy cost to create an interface between α and β. Our theory is invariant under the simultaneous exchange of labels: A ↔ C, a ↔ c; so $\Delta f_a = \Delta f_c \equiv \Delta f$. The free energy densities of the structures are ordered in the following way, depending on the value of Δf:

$$\Delta f < 0: \quad f_{PS} > f_{CSDL} > f_{NCS} \tag{20}$$

$$\Delta f > 0: \quad f_{NCS} > f_{CSDL} > f_{PS} \tag{21}$$

$$\Delta f = 0: \quad f_{NCS} = f_{CSDL} = f_{PS} \tag{22}$$

Our results suggest that below the triple point $\Delta f < 0$, above the triple point $\Delta f > 0$, and at the triple point $\Delta f = 0$.[23] We also observe that, near the triple point, f_{CSDL} lies approximately halfway between f_{NCS} and f_{PS} as eqs 17 and 18 with $\Delta f_a = \Delta f_c \equiv \Delta f$ predict.

In the experiments of ref 4, performed with symmetric block compositions and $\Omega = 1.5$, two-phase coexistence between a NCS phase and a triblock-rich phase was observed for $\bar{\phi}_2 \approx 0.18$, while for $\bar{\phi}_2 \approx 0.4$ a predominantly NCS phase was observed. These results are consistent with the phase diagram in Figure 2. However, when comparing theory to experiment, it is important to note that it is likely that the experiments were performed in the strong segregation regime rather than in the intermediate segregation regime ($\chi N \approx 14$) where we predict the widest stability region for the NCS phase. Also, the assumption in Figure 2 of equal Flory−Huggins interaction parameters does not hold for the experiments. On the other hand, we have seen that the structure of the phase diagram is insensitive to slight variations of the Flory−Huggins interaction parameters, with the exception of an upward or downward shift in the widest region of NCS stability and the triple point. Thus, it is possible for the experiments to be performed at relatively strong segregation but still be below the triple point in the phase diagram. Also, although we cannot exclude the possibility that the experiments observed the pure NCS phase, it is likely, given the

narrow region of NCS stability, that the experiments were in the two-phase coexistence region and observed a predominance of NCS phase due to the proximity of the NCS stability region.

One possible experimental strategy for obtaining a pure NCS phase is to begin in the disordered phase with the blend composition tuned to the composition of the critical point (here $\bar{\phi}_2 \approx 0.35-0.4$) and then perform a shallow-temperature quench into the NCS stability region.[24] The quench should be as shallow as possible so as to minimize the influence of both kinetic effects and the intervening MCS region on the formation of the NCS phase. As we have shown in Figure 7, when $\chi_{AB} = \chi_{BC} > \chi_{AC}$, the region of MCS stability narrows as the MCS-to-NCS critical point moves to lower values of $\chi_{AC}N$, closer to the order−disorder transition. However, our preliminary investigation into the possibility of a direct transition from the disordered to NCS phase suggests that for a large relative repulsion between the triblock middle and outer blocks ($\chi_{AB} = \chi_{BC} = 1.5\chi_{AC}$) the NCS phase can become unstable to phase separation into triblock- and diblock-rich phases, while a narrow region of MCS stability remains. Thus, a compromise must be found between decreasing the width of the MCS region and maintaining the stability of the NCS phase.

IV. Conclusions

We have examined the phase behavior of blends of ABC triblock and ac diblock copolymers using self-consistent mean-field theory. A representative phase diagram is shown in Figure 2. For segregations just above the order−disorder transition the blend forms a centrosymmetric lamellar phase where the triblocks and diblocks mix together (the MCS phase). For stronger segregation (increased χN or increased Ω) the B block tends to expel the diblock a and c blocks from its domain. As a result, the triblocks and diblocks spatially separate by forming either alternating layers of triblock and diblock or a phase-separated state. In the former case, we observe a narrow region around $\bar{\phi}_2 \approx 0.4$ where a pure NCS lamellar phase (Figure 1c) is stable. In the latter case, we observe large regions of two-phase coexistence between the NCS phase and either a triblock-rich or a diblock-rich MCS phase, depending on the value of $\bar{\phi}_2$. The structure of this phase diagram is insensitive to slight variations in the relative values of the Flory−Huggins interaction parameters. The only effect is an upward (or downward) shift of the phase coexistence curve and the triple point. Such variations do not measurably effect the width of the NCS region.

For intermediate segregation, our results suggest that there is a second-order critical point where a continuous transition from the MCS phase directly to the NCS phase occurs. The order parameter for this transition is the amplitude of the odd-parity basis functions (sines) for the monomer profiles. As the segregation is increased, the region of stability for the NCS phase narrows to a sliver and terminates at a triple point. Above the triple point there is two-phase coexistence between almost pure triblock and diblock phases. This is the first work to suggest the existence of the critical point and the triple point in the phase diagram for this blend.

The phase diagram in Figure 2 is consistent with the experiments of Goldacker et al.,[4] who observed coexisting triblock-rich and NCS lamellae for $\bar{\phi}_2 \approx 0.18$ and a predominance of NCS lamellae for $\bar{\phi}_2 \approx 0.4$. The narrowness of the region of NCS stability suggests that careful adjustment of the blend parameters is necessary to observe the pure NCS phase. Our theory predicts that the width of the NCS stability region can be maximized by studying blends near the phase coexistence curve which have a triblock to diblock length ratio less than 1.5.

Earlier theoretical work by Leibler et al. [9] and Birshtein et al.[12] on these blends focused on the mechanism responsible for the stability of the NCS phase in the strong segregation limit. In ref 9 subtle entropic interactions arising from the asymmetric interpenetration of a and A blocks from the diblock and triblock, respectively, cause the system to favor mixed aA domains over AA and aa domains (the same mechanism favors cC domains over CC and cc domains) and lead to a stable NCS phase. In ref 12 it is the different grafting densities of the brush coming from the triblock and the brush coming from the diblock that favor mixed aA and cC domains. Our work complements this earlier work since we can examine the blend phase diagram without the need to assume the strong segregation limit. However, in contrast to refs 9 and 12, our calculations show that the NCS phase is only stable for intermediate segregation and that for strongly segregated blends there is two-phase coexistence between triblock-rich and diblock-rich phases. A reconciliation between our results and those of refs 9 and 12 in the strong segregation regime is necessary. A clue to the nature of the entropic interaction driving the stability of the NCS phase is our observation that the region of NCS stability roughly corresponds to eq 16, the condition for there to be equal numbers of triblock and diblock copolymers in the two polymer brushes composing the aA and cC domains. It would be interesting to examine the interpenetration of the triblock and diblock chain profiles in the aA and cC domains using self-consistent mean-field theory. This would allow a more direct comparison to be made with the theories of refs 9 and 12. It may be that with increasing segregation the chain interpenetration in the aA and cC domains becomes more symmetric and the brush grafting densities more similar, reducing the stability of the NCS phase in the strong segregation regime and leading to the triple point seen in Figure 2. An analytical calculation of the stability of the MCS phase toward the NCS phase, near the critical point, may also be illuminating.

Only lamellar structures are considered in this study. Even though we have been careful to select parameters that favor the lamellar phase, it is possible that stable nonlamellar structures exist in our phase diagram.[25] (Some observations of nonlamellar structures in these blends are discussed in ref 7.) We can however say that, for the parameters examined, the size of the region of NCS stability is the *maximum* possible. Also, we have ignored composition fluctuations in the present mean-field treatment. Fluctuations may modify some of the detailed structure of the phase diagram, especially near the critical point, but we believe a region (perhaps a smaller one) of NCS stability will survive the effects of composition fluctuations.

Acknowledgment. The authors thank Prof. Hugh Couchman for access to his computing resources and Mr. David Cooke for helpful suggestions with coding. They also thank Dr. François Drolet for using his combinatorial method to confirm the phases observed in Figure 2 and Profs. Michael Schick, David Morse, and Thomas

P. Russell for useful comments. This work was supported by the Natural Sciences and Engineering Research Council of Canada.

References and Notes

(1) Petschek, R. G.; Wiefling, K. M. *Phys. Rev. Lett.* **1987**, *59*, 343−346.
(2) Tournilhac, F.; Blinov, L. M.; Simon, J.; Yablonsky, S. V. *Nature* **1992**, *359*, 621−623.
(3) Stupp, S. I.; LeBonheur, V.; Walker, K.; Li, L. S.; Huggins, K. E.; Keser, M.; Amstutz, A. *Science* **1997**, *276*, 384−389.
(4) Goldacker, T.; Abetz, V.; Stadler, R.; Erukhimovich, I.; Leibler, L. *Nature* **1999**, *398*, 137−139. Goldacker, T.; Abetz, V.; Stadler, R. *Macromol. Symp.* **2000**, *149*, 93−98.
(5) NCS phases have also been observed in blends of two triblock copolymers (see ref 7).
(6) Zheng, W.; Wang, Z.-G. *Macromolecules* **1995**, *28*, 7215−7223.
(7) Abetz, V.; Goldacker, T. *Macromol. Rapid Commun.* **2000**, *21*, 16−34.
(8) An exception is the helical structure, discussed by: Krappe, U.; Stadler, R.; Voigt-Martin, I. *Macromolecules* **1995**, *28*, 4558−4561.
(9) Leibler, L.; Gay, C.; Erukhimovich, I. *Europhys. Lett.* **1999**, *46*, 549−554.
(10) In addition to (...ABCcaacCBA...), another possible centrosymmetric double-layer configuration is (...CBAaccaABC...). In this paper the molecular parameters are chosen such that the theory is invariant under simultaneous interchange of the labels A ↔ C and a ↔ c (only the results mentioned in ref 23 do not have this invariance). Thus, these two configurations are equivalent.
(11) When both the energies of formation of AA, aa, and aA domains are equal and the energies of formation of CC, cc, and cC domains are equal, the possibility exists to form lamellar phases with random sequences of triblock and diblock.[4] Random sequences are beyond the scope of this paper, however, and will not be considered.
(12) Birshtein, T. M.; Polotsky, A. A.; Amoskov, V. M. *Macromol. Symp.* **1999**, *146*, 215−222. Amoskov, V. M.; Birshtein, T. M.; Pryamitsyn, V. A. *Macromolecules* **1998**, *31*, 3720−3730.
(13) Shi, A.-C.; Noolandi, J. *Macromolecules* **1994**, *27*, 2936−2944.
(14) Helfand, E. *J. Chem. Phys.* **1975**, *62*, 999−1005. Hong, K. M.; Noolandi, J. *Macromolecules* **1981**, *14*, 727−736.
(15) Matsen, M. W. *Phys. Rev. Lett.* **1995**, *74*, 4225−4228.
(16) Matsen, M. W.; Schick, M. *Phys. Rev. Lett.* **1994**, *72*, 2660−2663.
(17) Shi, A.-C.; Noolandi, J.; Desai, R. C. *Macromolecules* **1996**, *29*, 6487−6504.
(18) Laradji, M.; Shi, A.-C.; Noolandi, J.; Desai, R. C. *Macromolecules* **1997**, *30*, 3242−3255.
(19) The diblock chemical potential μ_2 and the average diblock volume fraction ϕ_2 are related via the free energy density f through $\bar{\phi}_2 = -\partial f/\partial \mu_2$.
(20) For example, for the NCS structure with $\chi N = 30$ it was found that 25 cosines and 25 sines are necessary to achieve an accuracy of 10^{-6}; for $\chi N = 15$ it was found that 15 cosines and 15 sines are sufficient.
(21) Similar mixed structures have been studied in blends of ABC triblock and AB diblock copolymers: Birshtein, T. M.; Zhulina, E. B.; Polotsky, A. A.; Abetz, V.; Stadler, R. *Macromol. Theory Simul.* **1999**, *8*, 151−160.
(22) Kittel, C.; Kroemer, H. *Thermal Physics*; W. H. Freeman and Co.: New York, 1980.
(23) We have performed a preliminary survey of the phase diagram for the case where all the Flory−Huggins interaction parameters are different ($\chi_{AB} = 1.1\chi_{AC}$, $\chi_{BC} = 0.9\chi_{AC}$), which breaks the invariance of the blend under the simultaneous exchange of the labels: A ↔ C, a ↔ c. Our results suggest that, in this case, the CSDL phase can become stable (and the NCS phase metastable) with increasing segregation, but before the triple point is reached. However, in this phase diagram the possibility for nonlamellar phases complicates the interpretation.
(24) Russell, T. P., private communication.
(25) The combinatorial method of Drolet and Fredrickson [Drolet, F.; Fredrickson, G. H. *Phys. Rev. Lett.* **1999**, *83*, 4317−4320], which does not assume a priori a particular space group when solving the self-consistent mean-field equations, has been applied to the situation in Figure 2 (Drolet, F., private communication). The results are consistent with the phases and phase diagram observed in Figure 2. In particular, they suggest that diblocks and triblocks with symmetric chain compositions and equal Flory−Huggins interaction parameters order into lamellar morphologies.

MA010601Q